5-2

Drift-Diffusion-Based Modeling of the Non-Quasistatic Small-Signal Response for RF-MOSFET Applications

H. Ueno, S. Jinbou, H. Kawano, *K. Morikawa, N. Nakayama,
M. Miura-Mattausch, and *H. J. Mattausch

Graduate School of Advanced Sciences of Matter, *Research Center for Nanodevices and Systems,
Hiroshima University, 1-3-1, Kagamiyama, Higashi-Hiroshima, 739-8526, Japan
Phone: +81-824-24-7637 Fax: +81-824-22-7195 E-mail: jinbou@hiroshima-u.ac.jp

Abstract — **A non-quasistatic MOSFET model for the small-signal response is developed by including the continuity equation in an analytical way. This model developed basing on the drift-diffusion approximation enables to predict the high-frequency response for any bias conditions. Our result shows that the quasistatic approximation calculates the response approximately correct up to $f_T/2$, which is much higher than $f_T/10$ previously estimated.**

I. Introduction

Technology development for scaling the gate length (L_g) down to 100nm regime promises to accomplish RF-applications of MOSFETs. Correct modeling of small-signal high frequency characteristics is an urgent task for utilizing the accomplishment. This requires the extension of the quasistatic (QS) approximation assumed for circuit simulation to the non-quasistatic (NQS) level considering the carrier transit time in the channel. There are two approaches developed for the extension. One is based on the equivalent circuit including components describing the carrier response phenomenologically [1]. The other is to consider the continuity equation explicitly [2]. However, both approaches have still shortcomings. The equivalent circuit model cannot know exactly, whether the NQS effect is correctly included. Whereas inclusion of the continuity equation is developed based on the drift approximation, which is not sufficient for advanced MOSFET applications with reduced bias condition as demonstrated in Fig. 1. For lower power consumption, the reduced L_g devices are required, which can keep the higher cut-off frequency (f_T) under the moderate inversion regime, where both drift and diffusion contributions are important. Thus, the purpose of this work is to develop a model including the continuity equation under the drift-diffusion approximation [3]. This allows to estimate the NQS effect correctly, and we can exploit the result to develop correct equivalent circuit model for RF-circuit simulation.

II. Model Formulation

We solve the current density equation and the continuity equation analytically. The drift-diffusion approximation describes the drain current (I_{ds}) as a function of the surface potential at source and drain side (ϕ_{S0} and ϕ_{SL}) obtained by solving the Poisson equation iteratively [4]:

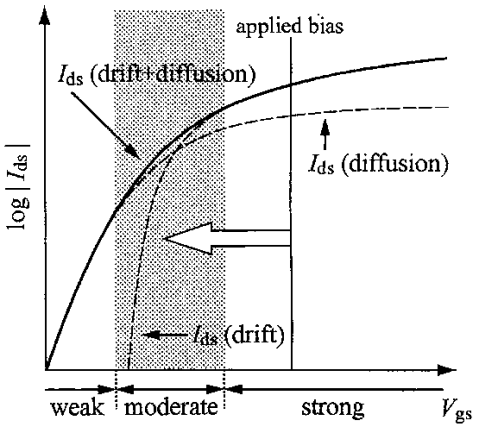

Fig. 1: Partitioning of I_{ds} into the drift and diffusion components. The shadow region represents the moderate inversion region in which the diffusion component cannot be neglected. The white arrow indicates the reduction of applied bias according to the technology generations.

$$I_{ds} = \frac{W}{L}\mu\frac{IDD}{\beta} \qquad \left(\beta = \frac{q}{kT}\right)$$

$$\begin{aligned} IDD = {} & C_{ox}(\beta V'_G + 1)(\phi_{SL} - \phi_{S0}) - \frac{\beta}{2}C_{ox}(\phi_{SL}^2 - \phi_{S0}^2) \\ & - \frac{2}{3}\left(qN_{sub}L_D\sqrt{2}\right)\left[\{\beta(\phi_{SL} - V_{bs}) - 1\}^{3/2}\right. \\ & \qquad \left. - \{\beta(\phi_{S0} - V_{bs}) - 1\}^{3/2}\right] \\ & + \left(qN_{sub}L_D\sqrt{2}\right)\left[\{\beta(\phi_{SL} - V_{bs}) - 1\}^{1/2}\right. \\ & \qquad \left. - \{\beta(\phi_{S0} - V_{bs}) - 1\}^{1/2}\right] \qquad (1) \\ & (V'_G = V_{gs} - V_{fb} - \Delta V_{th}) \end{aligned}$$

where C_{ox} is the oxide capacitance, N_{sub} the substrate doping concentration, L_D the Debye length, V_{fb} the flat-band voltage, ΔV_{th} the threshold voltage deviation from the long-channel device, respectively. With the current equation, the continuity equation derives small-signal current responses. Y-parameter components are derivatives of the small-signal currents.

Derived final equations for the Y-parameter compo-

nents are written by series of polynomial functions of frequency (f):

$$Y_{gg} = \left[\frac{2}{3}g_m s\frac{1+4\alpha+\alpha^2}{(1+\alpha)^2} + \frac{2}{45}g_m s^2 \cdot\frac{2+11\alpha+2\alpha^2}{(1+\alpha)^3}\cdots\right]\frac{1}{D} \quad (2)$$

$$Y_{dg} = \left[g_m - \frac{2}{3}g_m s\frac{\alpha(\alpha+2)}{(1+\alpha)^2} - \frac{2}{45}g_m s^2 \cdot\frac{\alpha(5+8\alpha+2\alpha^2)}{(1+\alpha)^4}\cdots\right]\frac{1}{D} \quad (3)$$

$$D = 1 + \frac{4}{15}s\frac{1+3\alpha+\alpha^2}{(1+\alpha)^3} + \frac{1}{45}s^2\frac{1+4\alpha+\alpha^2}{(1+\alpha)^4}\cdots$$

$$s = j2\pi f\frac{LW}{g_m}\frac{\partial Q_{i0}}{\partial V_{gs}}$$

$$\alpha = 1 - C_{ox}\frac{(1+\delta)(\phi_{SL}-\phi_{S0})}{Q_{i0}}$$

$$\delta = 2\frac{\sqrt{2}qN_{sub}L_D}{C_{ox}}\left\{\left[\frac{2}{3}\beta^2(\phi_{SL}-\phi_{S0})^2 + 2\beta(\phi_{SL}-\phi_{S0}) \cdot(\beta(\phi_{S0}-V_{bs})-1) + 2(\beta(\phi_{S0}-V_{bs})-1)^2\right] \Big/ \left[(\beta(\phi_{SL}-V_{bs})-1)^{3/2} + (\beta(\phi_{S0}-V_{bs})-1)^{3/2}\right] - (\beta(\phi_{S0}-V_{bs})-1)^{1/2}\right\}/(\phi_{SL}-\phi_{S0})$$

where Q_{i0} is the inversion charge density at source side. Thus each term of the series consists of coefficients determined by the surface potentials in stead of applied biases as with the conventional drift approximation [2]. Our model is linked with the circuit simulation model HiSIM (Hiroshima-university STARC IGFET Model) [5], providing the surface potential values as well as device parameter values required for the Y-parameter calculation.

III. Results

Fig. 2 shows comparison of measured Y-parameter characteristics (Y_{gg} and Y_{dg}) with calculated results based on an equivalent-circuit-model approach with HiSIM [6]. The NQS effect is included with the Elmore resistances [7]. The agreement is quite well up to f_T. Fig. 3 shows the same calculation as shown in Fig. 2 but without the extrinsic capacitances and resistances from the equivalent circuit by symbols. To focus only on the carrier response in the channel, we perform further simulations under this condition. Fig. 3 depicts also calculated Y_{gg} and Y_{dg} with the developed NQS model. The result demonstrates that the developed NQS model describes the response characteristics of a real intrinsic device correctly. However, deviations between the two models (equivalent circuit and NQS with inclusion of the continuity equation) become serious for large f. The reason may be attributed to the limitation of the Elmore resistances introduced to describe the NQS effect phenomenologically.

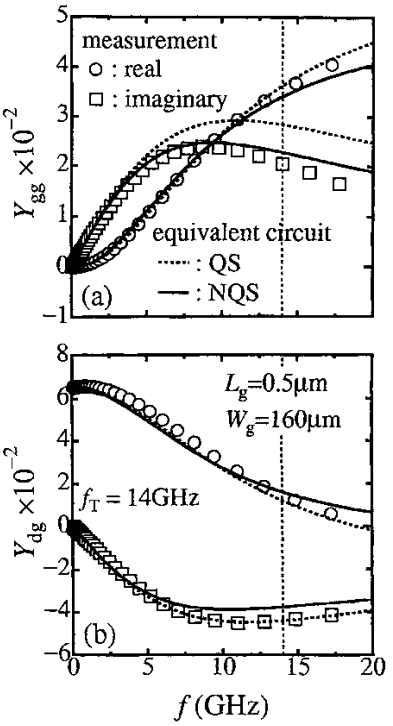

Fig. 2: Comparison of calculated Y-parameters ((a) Y_{gg} and (b) Y_{dg}) by the QS (dashed curves) and NQS (solid curves) equivalent circuit models with measured data (symbols) for $L_g = 0.5\mu$m and $W_g = 160\mu$m at V_{gs} giving maximum g_m ($V_{gs} - V_{th} = 1.0$V and $V_{ds} = 1.2$V). The vertical dashed line indicates the cut-off frequency f_T.

Fig. 4 compares calculated Y-parameters with our NQS model and the conventional model based on the drift approximation under the moderate inversion condition. As the I_{ds} description based on the drift approximation, we use the well-known description [1] by approximating $\phi_{S0} = 2\Phi_B$ and $\phi_{SL} = 2\Phi_B + V_{ds}$ in Eq. (1).

$$I_{ds} = \frac{W}{L}\mu C_{ox}\frac{(V_{gs}-V_{th})^2}{2(1+\delta)}(1-\alpha)^2 \quad (4)$$

$$\begin{cases}\alpha = 1 - \dfrac{(1+\delta)V_{ds}}{V_{gs}-V_{th}} & \text{for } V_{ds} \le \dfrac{V_{gs}-V_{th}}{1+\delta} \\ \alpha = 0 & \text{for } V_{ds} > \dfrac{V_{gs}-V_{th}}{1+\delta}\end{cases}$$

$$V_{th} = V_{fb} + 2\Phi_B + \frac{\sqrt{2\epsilon_{Si}qN_{sub}}}{2C_{ox}}\sqrt{2\Phi_B}$$

$$\delta = \frac{\sqrt{2\epsilon_{Si}qN_{sub}}}{2C_{ox}\sqrt{2\Phi_B - V_{bs}}}$$

A clear difference is that the f dependence of the imaginary parts in Y_{gg} and Y_{dg} are steeper for the drift approximation. The main cause of the different response characteristics is due to different features of two extracted device parameters (mobility μ and gate intrinsic capaci-

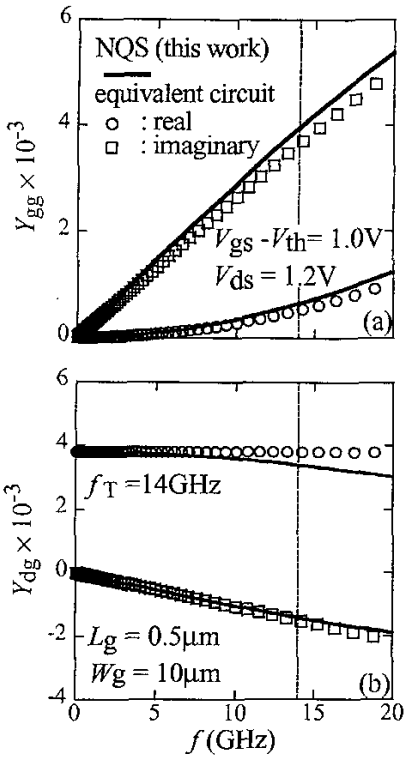

Fig. 3: Symbols are calculated results with the NQS equivalent circuit model shown in Fig. 2 but excluding extrinsic capacitances and resistances. Solid curves are calculated results with the developed NQS model.

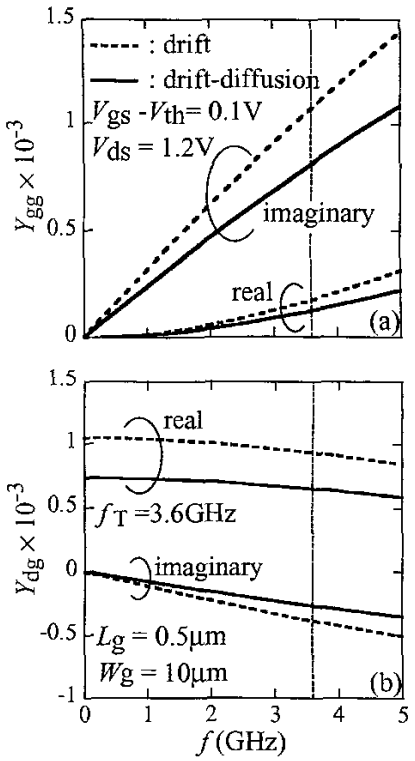

Fig. 4: Comparison of Y-parameters calculated by the NQS model based on the drift-diffusion approximation (solid curves) with that based on the drift approximation (dashed curves) at $V_{gs} - V_{th} = 0.1$V.

tance C_{int}) as demonstrated in Fig. 5. With the drift approximation, device parameters do not reflect the physically correct device characteristics below strong inversion and there is a non-consistency between the current and capacitance characteristics. On the other hand, with the drift-diffusion approximation, the consistency between the current and capacitance characteristics are preserved under the moderate inversion condition because of the surface potential based calculation. Fig. 6a shows the comparison of the low-frequency C_{gg} estimated from the imaginary part of Y_{gg} with the drift and the drift-diffusion approximation. The C_{gg} characteristics calculated by HiSIM independently are also depicted. Fig. 6b shows the comparison of I_{ds} with the drift and drift-diffusion approximation. Although the I_{ds} characteristics roughly coincide each other, C_{gg} characteristics estimated from the calculated Y_{gg} characteristics are different. Though the results with the drift approximation derivate, those with the drift-diffusion approximation agree well with those calculated by HiSIM directly. Even though the deviation of the drift model becomes smaller in the strong inversion regime, an obvious deviation still exists.

Fig. 7 shows a comparison of calculated Y_{gg} and Y_{dg} based on the drift-diffusion-approximation with the NQS

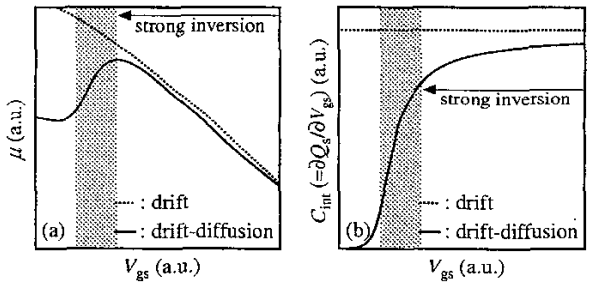

Fig. 5: Comparison of extracted device parameters (a) mobility μ and (b) intrinsic capacitance C_{int} with the drift-diffusion approximation (solid curves) and with the drift approximation (dotted curves). The shadowed areas indicate the moderate inversion region.

and QS models. The QS approximation describes simply [8]

$$Y_{gg} = j\,2\pi f C_{gg} \tag{5}$$

$$Y_{dg} = g_m - j\,2\pi f(C_m + C_{gd}) \tag{6}$$

where C_m is the transcapacitance [1]. Of course deviations between the models are obvious, however, inter-

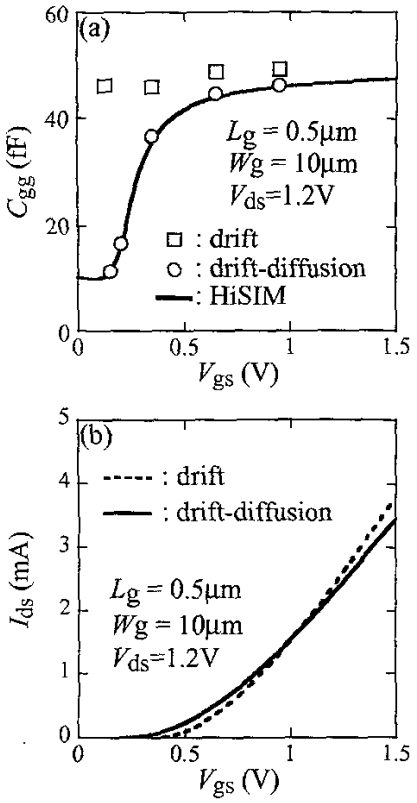

Fig. 6: (a) Estimated low-frequency C_{gg} from the imaginary part of Y_{gg} with drift (open squares) and drift-diffusion approximation (open circles). C_{gg} characteristics calculated by HiSIM are shown by solid curve. (b) Calculated I_{ds} with drift (dashed curve) and drift-diffusion approximation (solid curve).

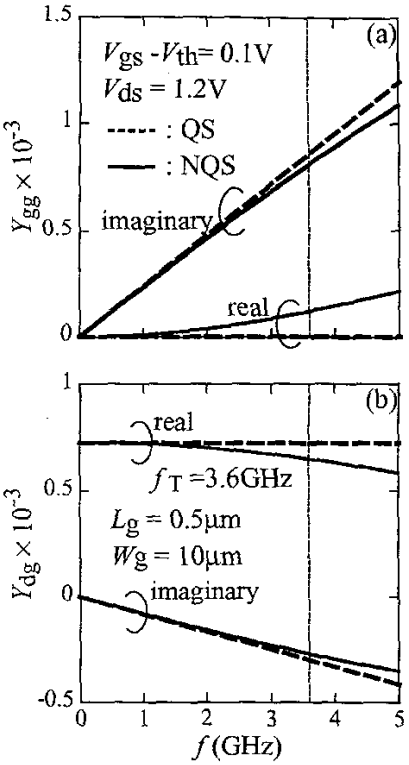

Fig. 7: Calculated Y-parameter values with the NQS model (solid curves) and the QS model (dashed curves).

esting features are recognized. The calculated imaginary parts, determining the capacitive component of the response, are accurate enough up to f_T with the QS model. Whereas the real parts, determining the conductive response, provide sufficient accuracy only up to $f_T/2$. These findings are true, if all device parameters required for the calculation are correctly determined. The result reminds us of the fact that the NQS effect is due to the delay of the carrier response for high-frequency operation.

IV. Conclusion

We have developed a NQS model for Y-parameters based on the drift-diffusion approximation by solving the current density equation and the continuity equation analytically. Our result shows that the larger contribution of the NQS effect is observed rather in the real part of the Y-parameter values, describing the conductive carrier response. Nevertheless, the QS model is accurate enough up to $f_T/2$, which is substantially more than $f_T/10$ predicted previously [1].

References

[1] Y. Tsividis, "Operation and Modeling of the MOS Transistor," 2nd ed., *New York, McGraw-Hill*, 1999.

[2] J. J. Paulos and D. A. Antoniadis, *IEEE Electron Dev. Lett.*, vol. EDL-4, no. 7, pp. 221–224, 1983.

[3] J. R. Brews, *Solid-State Electron.*, vol. 21, pp. 345–355, 1978.

[4] M. Miura-Mattausch, U. Feldmann, A. Rahm, M. Bollu, and D. Savignac, *IEEE Trans. CAD/ICAS*, vol. 15, pp. 1–7, 1996.

[5] HiSIM User's Manual

[6] H. Kawano, M. Nishizawa, S. Matsumoto, S. Mitani, M. Tanaka, N. Nakayama, H. Ueno, M. Miura-Mattausch, and H. J. Mattausch, *International Microwave Symposium Digest*, vol. 3, pp. 2121–2124, 2002.

[7] W. C. Elmore, *J. Appl. Phys.*, vol. 19, pp. 55–63, 1948.

[8] C. C. Enz and Y. Cheng, *IEEE Trans. Solid-State Circ.*, vol. 35, no. 2, pp. 186–201, 2000.